Talanta 94 (2012) 263–270

Contents lists available at SciVerse ScienceDirect

Talanta

journal homepage: www.elsevier.com/locate/talanta

Highly-sensitive cholesterol biosensor based on platinum–gold hybrid functionalized ZnO nanorods

Chengyan Wang [a], Xingrong Tan [b], Shihong Chen [a,*], Ruo Yuan [a,*], Fangxin Hu [a], Dehua Yuan [a], Yun Xiang [a]

[a] Education Ministry Key Laboratory on Luminescence and Real-Time Analysis, Key Lab of Chongqing Modern Analytical Chemistry, College of Chemistry and Chemical Engineering, Southwest University, Chongqing 400715, China
[b] Department of Endocrinology, 9th People's Hospital of Chongqing, Chongqing 400700, China

ARTICLE INFO

Article history:
Received 29 December 2011
Received in revised form 20 March 2012
Accepted 22 March 2012
Available online 29 March 2012

Keywords:
Multiwalled carbon nanotubes
Gold/platinum hybrid
Zinc oxide nanorods
Cholesterol oxidase
Biosensor

ABSTRACT

A novel scheme for the fabrication of gold/platinum hybrid functionalized ZnO nanorods (Pt–Au@ZnONRs) and multiwalled carbon nanotubes (MWCNTs) modified electrode is presented and its application for cholesterol biosensor is investigated. Firstly, Pt–Au@ZnONRs was prepared by the method of chemical synthesis. Then, the Pt–Au@ZnONRs suspension was dropped on the MWCNTs modified glass carbon electrode, and followed with cholesterol oxidase (ChOx) immobilization by the adsorbing interaction between the nano-material and ChOx as well as the electrostatic interaction between ZnONRs and ChOx molecules. The combination of MWCNTs and Pt–Au@ZnONRs provided a favorable environment for ChOx and resulted in the enhanced analytical response of the biosensor. The resulted biosensor exhibited a linear response to cholesterol in the wide range of 0.1–759.3 μM with a low detection limit of 0.03 μM and a high sensitivity of 26.8 μA mM^{-1}. The calculated apparent Michaelis constant K_M^{app} was 1.84 mM, indicating a high affinity between ChOx and cholesterol.

1. Introduction

As is known to all, normal concentration of cholesterol in human serum is in the range of 1.3–2.6 mg mL^{-1}, of which ~30% is sterol and ~70% is esterified with fatty acids [1]. High cholesterol accumulation in blood serum is strongly correlated with many clinical diseases, such as coronary disease, arteriosclerosis, myocardial infarction, brain thrombosis, lipid metabolism dysfunction, hypertension and so on [2]. Therefore, the determination of cholesterol levels in the blood of human is of great importance in clinical analysis/diagnosis.

In the analytical practice for the cholesterol measurement, high-performance liquid chromatography (HPLC) and gas chromatography (GC) are used frequently, but a very intensive pre-treatment of the samples is needed [3]. As for colorimetry, the method is simple, rapid and capable of being automated, but does require a large amount of serum sample [4]. With regard to spectrophotometry, non-selective and non-sensitive detection as well as the long response time limits its application. As another well-known biochemical detection method for cholesterol, electrochemical technique offers high performance detection as well as simplicity [5]. Because of their low detection limit, rapid response and low cost, amperometric biosensors are more promising than other electrochemical detection. To the amperometric cholesterol biosensors, the enzymatic reactions in the use of cholesterol oxidase (ChOx) as a receptor can be described as follows:

$$\text{Cholesterol} + O_2 \xrightarrow{\text{ChOx}} \text{Cholest} - 4 - \text{en} - 3 - \text{one} + H_2O_2$$

The cholesterol is oxidized by oxygen in the presence of ChOx and H_2O_2 is produced at the same time [6]. The electro-oxidation current of H_2O_2 is detected to determine the concentration of the cholesterol in the sample.

Owing to the unique properties such as good electrical conductivity, strong adsorptive ability and excellent biocompatibility, carbon nanotubes (CNTs) have been widely used in the region of biosensor [7]. Previous studies have indicated that CNTs had fast electron-transfer kinetics and could catalyze the electrochemical reaction of NADH [8], glucose [9,10], neurotransmitters [11], dopamine [12] and so on. Li group reported carbon nanotube modified biosensor for monitoring total cholesterol in blood, and the research stated clearly that CNTs modification not only promoted the electron transfer and almost doubled the sensitivity, but also improved the linearity of the electrode [13]. However, the poor solubility of CNTs in most solvents is one of the limitations in the design of CNT-based biosensing devices. Chitosan (CS), a natural cationic biopolymer, has attracted much interest owing to its interesting properties such as biocompatibility, non-toxicity, low-cost, good film forming ability, high mechanical strength and high

* Corresponding author. Tel.: +86 23 68253172; fax: +86 23 68253172.
E-mail addresses: cshong@swu.edu.cn (S. Chen), yuanruo@swu.edu.cn (R. Yuan).

0039-9140/$ – see front matter © 2012 Elsevier B.V. All rights reserved.
http://dx.doi.org/10.1016/j.talanta.2012.03.037

hydrophilicity [14]. It was usually used as a medium for dispersing multiwalled carbon nanotubes (MWCNTs) in aqueous solution. And the CS-MWCNTs dispersion solutions could keep homogeneous for several months. In the construction of biosensors, the CS-MWCNTs composite is usually combined with other nanoparticles such as Au, Ag, Pt, Cu, TiO_2, SiO_2, ZrO_2 and so on. Recently, some cholesterol biosensors based on CS-MWCNTs have been reported. Tan et al. [15] used sol–gel CS/SiO_2 and MWCNTs composite film to immobilize ChOx for detecting cholesterol and the performance of the biosensor with MWCNTs is superior to the biosensor without MWCNTs. Solanki et al. [16] immobilized cholesterol esterase (ChEt) and ChOx onto SiO_2-CS/MWCNTs bionanocomposite film for the detection of total cholesterol and the linearity of 10–500 mg/dL^{-1} is only two orders. Tsai et al. [6] fabricated amperometric cholesterol biosensor based on CNTs-CS-Pt-ChOx nanobiocomposite. The sensitivity of 44 mAM^{-1} cm^{-2} is higher than some other cholesterol biosensors, however, the stability of the prepared cholesterol biosensor was disappointed.

Zinc oxide (ZnO) is an n type semiconductive material with wide energy leap (Eg = 3.37 eV) and large exciton binding ability (60 meV) [17], and has useful electronic and optical properties. It has been demonstrated that both the size and shape or morphology have an influence on the properties of materials. Therefore, numerous attention has been paid to the synthesis of nanostructured ZnO such as nanoparticles [18], nanowires [19], nanobelts [20], nanorods [21], nanotubes [22] and hollow spheres [23] for various applications. ZnO nanorods have attracted considerable interest in the aspect of sensors due to many advantages, including large surface-to-volume ratio, excellent biological compatibility, high electron-transfer rates, non-toxicity and bio-safety. Notably, ZnO with a high isoelectric point (IEP ~9.5) is suitable for the adsorption of low IEP proteins or enzyme. Positively charged ZnO nanorods matrix not only provided a friendly microenvironment for the negatively charged proteins or enzyme to retain its activity but also promoted the direct electron transfer between the enzyme and the electrode to a large extent [24]. Zhang [24] et al. immobilized uricase on ZnO nanorods for a reagentless uric acid biosensor. To improve the properties of ZnO, the combination of ZnO with the metal materials such as Au, Ag, Cu and Pt was reported in the past years. Doping in ZnO with the noble metals [25] offers an effective approach to enhance the properties of ZnO nanostructures, which is crucial for their practical applications especially for the construction of biosensor. Gong [26] et al. prepared a Cu-doped ZnO film by co-sputtering of Cu and ZnO and developed a highly sensitive CO gas sensor. Wang [27] et al. constructed a sensitive SPR biosensor based on ZnO–Au nanocomposites for the determination of rabbit IgG. Wang and Zheng [28] prepared a modified electrode through electrodepositing silver nanoparticles (AgNPs) on a ZnO film, which exhibited wide linear range and low detection limit for the quantitative analysis of H_2O_2. Ahmad [29] et al. synthesized Pt-incorporated fullerene-like ZnO nanospheres by codeposition of $ZnNO_3$ and $H_2PtCl_6{\cdot}6H_2O$ and applied it to develop a highly sensitive amperometric cholesterol biosensor. The metal-ZnO nanostructures built a favorable bridge for electron communication between the electrode and the detecting substrate. To obtain the metal-ZnO nanostructures, the common method is depositing the metal on the surface of ZnO.

The cholesterol biosensors based on MWCNTs [13,30,31], ZnO [32,33], Pt–ZnO nanocomposites [29], Pt-MWCNTs nanocomposites [6,34] have been reported continually, but these biosensors are witnessed by the narrow linear rang, high detection limit or low sensitivity, as well as the unsatisfactory stability. In this paper, Pt–Au@ZnONRs composite was synthesized by the method of multiple-step chemosynthesis and was combined with MWCNTs to construct a cholesterol biosensor. This system provides a new and promising platform for electrochemical devices due to the coupling of advantages of Pt, ZnONRs and MWCNTs. Firstly, ZnO with a high IEP (~9.5) is suitable for the adsorption of the low IEP enzyme (for instance ChOx, IEP = ~4.9), and the large surface-to-volume ratio of MWCNTs and Pt–Au@ZnONRs make for more ChOx immobilized. Secondly, MWCNTs and ZnONRs could retain the enzyme bioactivity and enhance the electron transfer between the active center of the enzyme and the electrode. Thirdly, Pt is a well-known catalyst that has a high catalytic activity for H_2O_2 electro-oxidation, and both MWCNTs and ZnONRs can catalyze the electro-oxidation of H_2O_2, which sharply improve the sensitivity of the biosensor.

2. Experimental details

2.1. Reagents

Cholesterol oxidase (EC 1.1.3.6, 28 U mg^{-1}), cholesterol, chitosan (CS, MW: 100,000–300,000, deacetylating grade: 70–85%), $H_2PtCl_6{\cdot}6H_2O$ (99.9%), Triton X-100, Nafion (5%) were purchased from Sigma-Aldrich (Shanghai) Trading Co., Ltd. MWCNTs (>95% purity) were obtained from Chengdu Organic Chemicals Co. Ltd. of the Chinese Academy of Science and purified by fluxing in concentrated nitric acid for 7 h prior to use. Tetraethoxysilane (TEOS), 3-aminopropyltriethoxysilane (APTES), trioctylamine, H_2O_2 solution (30%) and 2-propanol (99.9%) were supplied by Chemical Reagent Co., Shanghai, China. Zinc acetate, cobalt (II) acetate, ethanol, ammonia solution, sodium citrate, L-cysteine, ascorbic acid and uric acid were purchased from Chemical Regent Co. Chongqing, China. Nano-Au seed solution was prepared according to the literature [35]. A series of phosphate-buffered solutions (PBS) were prepared by mixing the solutions of 0.05 M KH_2PO_4, 0.05 M Na_2HPO_4 and the supporting electrolyte was NaCl (0.9%). Other chemicals were of analytical-reagent grade without further purification. The cholesterol stock solution was prepared in a 50 mL aqueous solution containing 1 mL of 2-propanol and 1 mL of Triton X-100 in a bath at 60 °C and then diluted with deionized water. Double-distilled water was used throughout this study.

2.2. Apparatus and measurements

The electrochemical experiments were performed at room temperature utilizing an electrochemical workstation (CHI660D) with a three-electrode configuration. A modified glassy carbon electrode (GCE, 4 mm in diameter) was used as the working electrode, with saturated calomel electrode (SCE) as the reference electrode, and platinum as the counter electrode. Transmission electron microscopy (TEM) was performed on a TECNAI 10 (PHILIPS FEI Co., The Netherlands). Atomic force microscopy (AFM) images of the films were achieved by scanning probe microscope (Vecco, USA). X-ray photoelectron spectroscopy (XPS) measurements were carried out with a VG Scientific ESCALAB 250 spectrometer, using Al KR X-ray (1486.6 eV) as the light source. All the electrochemical experiments were carried out at room temperature.

2.3. Cholesterol biosensor fabrication

2.3.1. Preparation of Pt–Au@ZnONRs

Zinc oxide nanorods (ZnONRs) were prepared as following: zinc acetate (0.2335 g) and cobalt acetate (0.01295 g) were mixed in a three-neck flask with trioctylamine (10 mL). The flask was rapidly heated to 300 °C with a condenser. The solids dissolved slowly as the temperature increased, and the color of the solution changed from clear to royal blue. The reaction was continued for 120 min and cooled down to room temperature. The green precipitate was washed several times with ethanol to remove any cobalt precursor, as well as any cobalt metal particles.

Amino modification of ZnONRs was carried out as following: ZnONRs (15 mg) were dispersed in a beaker (50 mL) with 2-propanol (10 mL) and ethanol (20 mL). Then 2.5 mL deionized water and 0.8 mL ammonia solution (25%) were then added into the mixture. Under continuous stirring, 25 μL APTES and 50 μL TEOS were added into the reaction solution. The reaction was allowed to continue for 8 h at room temperature to achieve amino function of nanostructures. Then, amino functioned ZnONRs were separated from the reaction medium by centrifugation at 5000 rpm for 10 min, washed several times and dried in vacuum.

Pt–Au@ZnONRs was obtained as following: in a typical synthesis, the amino functioned ZnONRs (15 mg, dispersed in 5 mL ethanol) were mixed with the fresh gold seed solution (50 mL). After the solution was stirred for 5 h, the resulting nanorods were collected by centrifugation and washed 3 times with deionized water, and then redispersed in 50 mL deionized water for further use. Finally, the obtained nanorods coated with Au-seed nanoparticles were heated to a boil, 2 mL of 1% H_2PtCl_6 and 3 mL of 1% sodium citrate were added, followed by the addition of 5 mL ascorbic acid, which served as a reductant for the reduction of H_2PtCl_6. After the mixture was heated for about 30 min, Pt–Au hybrid functionalized ZnO nanorods (Pt–Au@ZnONRs) was obtained due to the formation of Pt shell driven by the Au seeds acting as nucleation centers. The resulting solution was centrifuged 4 times and the precipitates were dried in vacuum.

2.3.2. Modification of the electrode

A 0.1% CS solution was prepared by dissolving 10 mg CS in 10 mL 1% acetate solution (pH 5.0). MWCNTs were dispersed into 0.1% CS solution with the aid of ultrasonic agitation to form a homogeneous CS-MWCNTs suspension (2.0 mg mL^{-1}). Prior to the modification, GCE was polished with the 0.3 μm and 0.05 μm alumina slurry, and then sonicated in deionized water and ethanol for 5 min, respectively. The CS-MWCNTs film modified electrode was prepared by casting 5 μL of CS-MWCNTs on the surface of GCE and drying under room temperature in the air. Next, 5 μL of Pt–Au@ZnONRs suspension (2.0 mg mL^{-1}) was dropped on the CS-MWCNTs/GCE. After dried in the air, the modified electrode was immersed in ChOx solution (2.0 mg mL^{-1}) prepared with 0.05 M PBS (pH 7.0) containing 0.9% NaCl for 8 h, next, rinsed and dried it. The final electrode is taken as ChOx/Pt–Au@ZnONRs/CS-MWCNTs/GCE. The similar procedures were employed to fabricate ChOx/CS-MWCNTs/GCE and ChOx/Pt–Au@ZnONRs/GCE. All resulted electrodes were stored at 4 °C when not in use. The procedure for preparing cholesterol biosensor is schematically shown in Scheme 1.

2.4. Experimental measurements

Electrochemical experiments were performed in a conventional electrochemical cell containing a three-electrode arrangement at room temperature. A 0.05 M PBS (pH 7.0) including 0.9% NaCl was used as the test solution. Amperometric measurements were carried out under stirred condition at room temperature with an applied potential of 0.45 V. All potentials were measured vs. SCE.

3. Results and discussion

3.1. XPS and TEM of Pt–Au@ZnONRs

X-ray photoelectron spectroscopy (XPS) analysis was used to characterize the chemical composition in the Pt–Au@ZnONRs nanocomposite. Fig. 1A–C shows the XPS spectra of C1s, N1s, O1s, and all of the binding energies are agreed with their internal references in the spectrum. Obviously, two peaks could be distinguished in the Si2p spectra (Fig. 1D): one with higher binding energy located at about 102.8 eV which is typical for the thermally grown SiO_2 [36], and the other with lower binding energy located at 98.7 eV which is associated with Si from the substrate [37]. The Zn2p spectrum in Fig. 1E shows a doublet whose binding energies are 1021.1 and 1044.9 eV and can be identified as $Zn2p_{3/2}$ and $Zn2p_{1/2}$ lines, respectively. The binding energy difference between the two lines is 23.8 eV, which is well lying within the standard reference value of ZnO [38]. Fig. 1F is the XPS signature of the Au4f doublet (83.7 and 87.4 eV for $4f_{7/2}$ and $4f_{5/2}$, respectively) corresponding to the binding energy of metallic Au. The peaks located around 70.3 eV and 74.2 eV, are due to metallic platinum for $4f_{7/2}$ and $4f_{5/2}$ states (Fig. 1G), which firmly affirmed that Pt–Au@ZnONRs can be obtained via the previous method.

The topographies of the ZnONRs and gold-platinum hybrid functionalized ZnONRs were investigated using transmission electron microscopy (TEM), respectively. As shown in Fig. 2A, a large quantity of straight and smooth nanorods was observed. The average diameter of the nanorods was about 18 nm, and their length was ranging from 50 nm up to 300 nm. After Pt shell was grown around the Au seeds particles by a one-step reduction of 'H_2PtCl_6 growth solution' and selective deposition of Pt on the ZnONRs surface driven by the Au seeds acting as nucleation centers, the gold-platinum hybrid modified ZnONRs were obtained and the corresponding TEM image was presented in Fig. 2B. As expected, a layer shell structure with many nanoparticles was clearly observed at the surface of ZnONRs, and the diameter of the composite is about twice as larger as that of ZnONRs.

3.2. AFM of the modified films

The atomic force microscopy (AFM) images of CS-MWCNTs, Pt–Au@ZnONRs/CS-MWCNTs and ChOx/Pt–Au@ZnONRs/CS-MWCNTs modified films were investigated. As shown in Fig. 2C, the AFM micrograph of CS-MWCNTs film presents clearly tubular structures of MWCNTs, which covers the entire surface of the substrate. After the assembly of the Pt–Au@ZnONRs on the CS-MWCNTs, although the AFM image of resultant film (Fig. 2D) still displays tubular structures, the micrograph is obviously

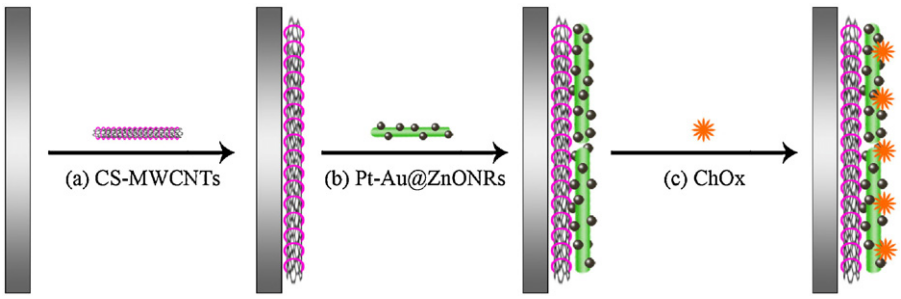

Scheme 1. The illustration of the preparation process of the cholesterol biosensor.

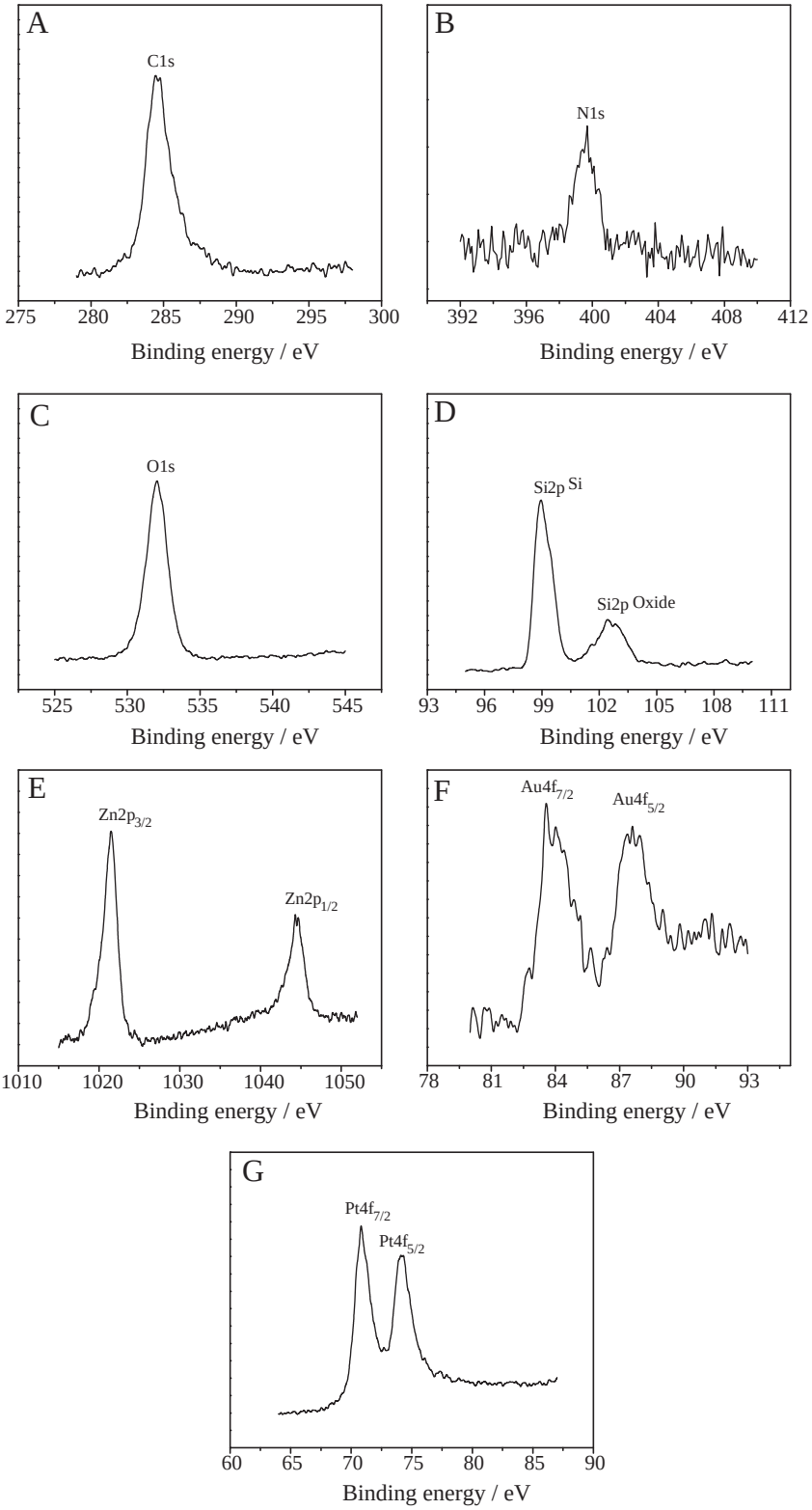

Fig. 1. XPS spectra of Pt–Au@ZnONRs: (A) C1s, (B) N1s, (C) O1s, (D) Si2p, (E) Zn2p, (F) Au4f and (G) Pt4f.

different from that of CS-MWCNTs because of following facts. On one hand, the tubular structure becomes shorter due to the difference in length between ZnONRs and MWCNTs. On the other hand, the tubular structure becomes relatively indistinct and the corresponding AFM image is characterized by many particles-like or island-like nanostructures, which is due to the modification of platinum–gold hybrid nanoparticles on the ZnONRs. In the case of ChOx/Pt–Au@ZnONRs/CS-MWCNTs film (Fig. 2E), the surface morphology becomes smooth, which might be ascribed to ChOx molecules filling the interstitial places between Pt–Au@ZnONRs and Pt–Au@ZnONRs, and Pt–Au@ZnONRs and MWCNTs, suggesting that ChOx is immobilized on the surface of the electrode.

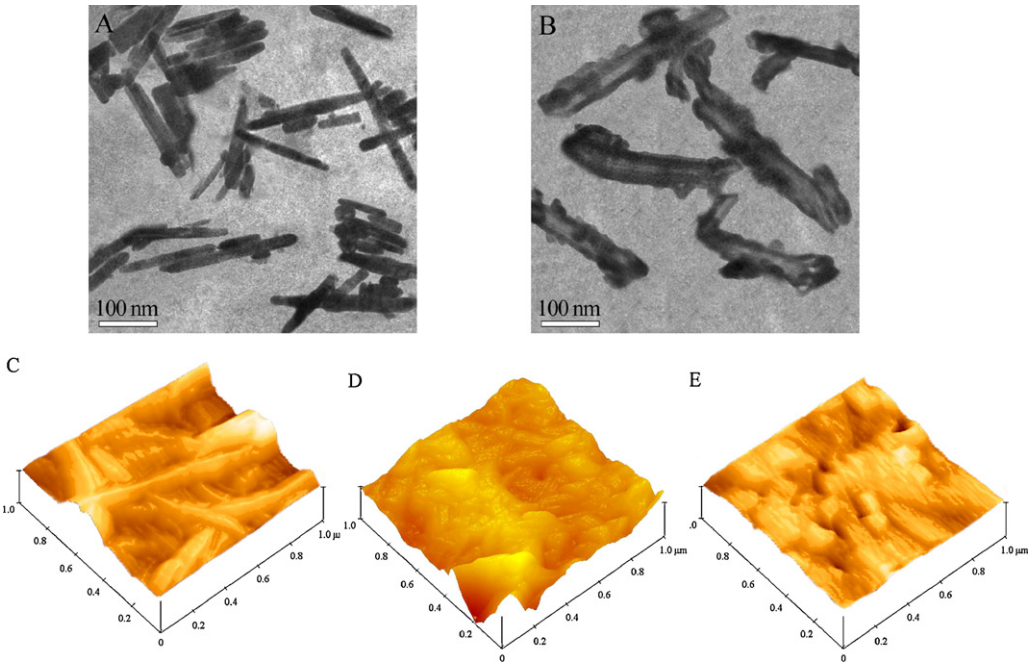

Fig. 2. TEM images of (A) ZnO nanorods and (B) Pt–Au@ZnONRs, AFM images of (C) CS-MWCNTs, (D) Pt–Au@ZnONRs/CS-MWCNTs and (E) ChOx/Pt–Au@ZnONRs/CS-MWCNTs films on the gold surface.

3.3. Electrochemical characterization of the biosensor

Fig. 3A shows the cyclic voltammograms (CVs) of (a) the bare GCE, (b) CS-MWCNTs/GCE, (c) Pt–Au@ZnONRs/CS-MWCNTs/GCE and (d) ChOx/Pt–Au@ZnONRs/CS-MWCNTs/GCE in 5.0 mM $[Fe(CN)_6]^{3-/4-}$ at scan rate of 50 mV s^{-1}. At the bare GCE, a pair of well-defined oxidation and reduction peaks of $[Fe(CN)_6]^{3-/4-}$ were observed (curve a). After the electrode was modified with CS-MWCNTs composite, an increase in peak current was observed (curve b). The reasonable explanation may be as follows. On the one hand, MWCNTs could form high electron conduction pathways between the electrode and the electrolyte, and obviously improve the diffusion of ferricyanide toward the electrode surface. On the other hand, positive charges of CS should be favorable for the approaching of ferricyanide anions, thus more $[Fe(CN)_6]^{3-/4-}$ would be attracted to the electrode surface modified with positively charged CS due to the electrostatic interaction, which led to an increase in peak current. Compared with curve b, the Pt–Au@ZnONRs/CS-MWCNTs/GCE gave an obvious larger peak current because of the good conductive property of Pt and Au. Furthermore, positively charged ZnONRs matrix also was favorable for the approaching of ferricyanide anions. When ChOx was assembled on the electrode, the peak current clearly decreased (curve d), indicating that the non-conductive ChOx was modified successfully.

Fig. 3B depicts the CVs of the proposed biosensor in 5.0 mM $[Fe(CN)_6]^{3-/4-}$ at different scan rates. It was observed that the peak currents are dependent on the scan rate in the range from 10 to 250 mVs^{-1}. In addition, the peak current vs. the square root of the scan rate plots (shown in the inset) exhibits a linear relationship, suggesting a diffusion-controlled process.

3.4. Optimization of experimental parameters for the biosensor

Fig. 4A shows the relationship between the chronoamperometric current response of the biosensor to 0.2 mM cholesterol and the potentials applied on the working electrode. The response current evidently increased from 0.2 to 0.6 V, which is due to the increase of electron transfer force. In order to avoid high working

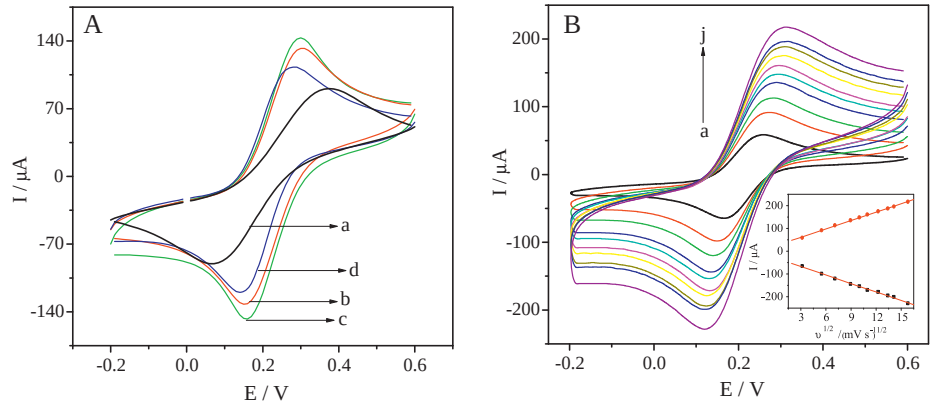

Fig. 3. (A) CVs of different modified electrodes in 5.0 mM $K_3[Fe(CN)_6]/K_4[Fe(CN)_6]$ (1:1). (a) bare GCE, (b) CS-MWCNTs/GCE, (c) Pt–Au@ZnONRs/CS-MWCNTs/GCE and (d) ChOx/Pt–Au@ZnONRs/CS-MWCNTs/GCE. Scan rate: 50 mV s^{-1}. (B) CVs of the ChOx/Pt–Au@ZnONRs/CS-MWCNTs/GCE in 5.0 mM $[Fe(CN)_6]^{3-/4-}$ (1:1) at various scan rates. From curve a to j corresponding to 10, 30, 50, 80, 100, 120, 150, 180, 200, 250 mV s^{-1}. Inset: The relationship between the peak currents and the square roots of the scan rates.

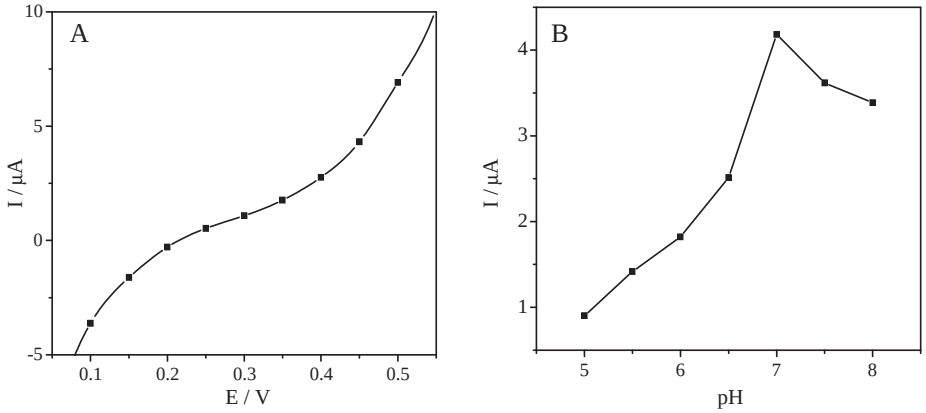

Fig. 4. Dependence of the current response of the cholesterol biosensor to 0.2 mM cholesterol (A) on the applied potential in pH 7.0 PBS and (B) on the pH of PBS at an applied potential of 0.45 V.

potential causing ascorbic acid and uric acid directly oxidized on the electrode surface while obtaining high sensitivity, the working potential of 0.45 V was appropriately used.

Since the activity of ChOx is affected by the pH of the PBS, the pH effect on the biosensor performance was investigated by measuring the chronoamperometric current response to 0.2 mM cholesterol at 0.45 V. As ZnO is a kind of amphoteric compound and not stable in both strong acid and base solutions, the pH dependence of the biosensor was evaluated in the range of pH 4.5–8.5 in this experiment. As clearly seen in Fig. 4B, the biosensor shows an optimal response at pH 7.0. All the amperometric experiments have been carried out in pH 7.0 PBS.

3.5. The response characteristics of the biosensor

Fig. 5 exhibits the CVs for ChOx/Pt–Au@ZnONRs/CS-MWCNTs/GCE without (curve a) and with 0.6 mM cholesterol (curve b) in 0.05 M PBS at pH 7.0 in the range of −0.2 to 0.6 V at scan rate of 50 mV s^{-1}. Compared to the CVs without cholesterol, the CVs in the presence of cholesterol shows the increase in both the anodic current and cathodic current, confirming the electrocatalytic response of ChOx/Pt–Au@ZnONRs/CS-MWCNTs/GCE to cholesterol.

Fig. 6A displays the amperometric response of the biosensor for the successive increase in cholesterol concentrations at an operating potential of 0.45 V in stirred PBS (pH 7.0). With

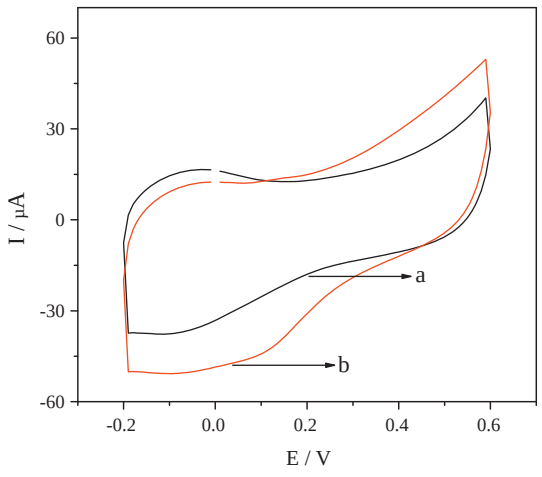

Fig. 5. CVs of the biosensor in 0.05 M PBS (pH 7.0) without cholesterol (a) and with 0.6 mM cholesterol (b) at the scan rate of 50 mV s^{-1}.

successively increasing concentration of cholesterol, the sensing currents increase steadily owing to the increased concentration of H_2O_2 produced during the enzymatic reaction. The current at the modified electrode increased immediately after the addition of cholesterol and reached a steady value. The average time required to reach 95% of the saturation current value was less than 6s. The response time at this biosensor is lower than those reported for the cholesterol biosensors based on MWCNTs/SiO_2-CS nanobiocomposite (10s) [16], polyaniline (PANI) films (40s) [39] and ChOx in sol–gel film (51s) [40] and as well as much lower than 5 min [41] and 12 min [42] reported for spectrophotometric method. This fast response is attributed to the synergetic influence of MWCNTs and Pt–Au@ZnONRs.

Fig. 6B shows the relation between the response current and cholesterol concentration for the fabricated biosensor. As seen, the response current increases as the concentration of cholesterol increases and saturates at high concentration of cholesterol. Under optimized conditions, the steady-state current of the fabricated biosensor showed a linear range of 0.1–759.3 μM, which was wider than 0.5–5 mM [43] for amperometric cholesterol biosensor, 2.6–15.6 mM [41] and 0.13–1.3 mM [42] for spectrophotometric method and 0.1–2.0 μM [44] for liquid chromatography with fluorescence. In the linear range, the sensitivity of the biosensor is estimated to be 26.8 μA mM^{-1}. Typically, ChEt-ChOx/MWCNTs/SiO_2-CS/ITO (3.8 μA mM^{-1}) [16], ChOx/PANI-MWCNTs/ITO (6.8 μA mM^{-1}) [45] and ITO/MWNTs(SH)-Au/CS-IL/ChOx (0.20 μA mM^{-1}) [43] biosensors show lower sensitivity than our presented biosensor. Based on the signal-to-noise ratio ($S/N = 3$), the detection limit of the fabricated cholesterol biosensor was estimated to be 0.03 μM, which is about four thousand times lower than 130 μM [41] and about ninety times lower than 2.6 μM [42] for spectrophotometric method. The apparent Michaelis–Menten constant (K_M^{app}), an indicator of the enzyme–substrate kinetics, can be estimated from the Lineweaver–Burk equation. The value of K_M^{app} is determined by analyzing the slope and intercept of the plot of the reciprocals of the steady-state current (I_{ss}) and the cholesterol concentration (C). Through linear regression equation $1/I_{ss}(\mu A^{-1}) = -0.05765 + 0.03135(1/C)(mM^{-1})$, K_M^{app} of the biosensor was estimated to be 1.84 mM, which is lower than ~4.7 mM for cholesterol biosensor based on Nafion/ChOx/ZnO [32] and 5 mM for cholesterol biosensor based on graphene-Pt nanoparticle [46]. From these results, we concluded that the proposed biosensor exhibits excellent performance in terms of response time, linear range, sensitivity, detection limit and K_M^{app}. This can be attributed to the following aspects. First of all, MWCNTs and Pt–Au@ZnONRs are favorable for the immobilization and retaining the enzyme

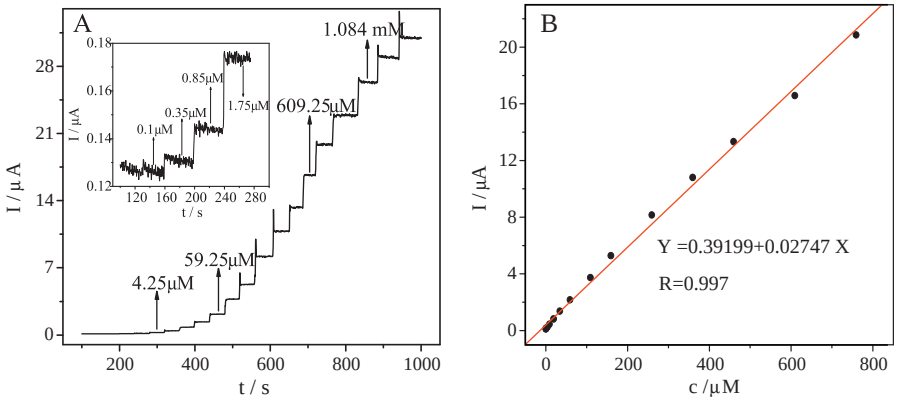

Fig. 6. (A) The current–time response of the biosensor to cholesterol upon successive additions of different concentrations cholesterol. Inset: The magnification of amperometric response of the biosensor to cholesterol from 100 s to 280 s. (B) The plot of the catalytic response current vs. cholesterol concentration.

bioactivity of ChOx molecule. Otherwise, the three components of Pt, MWCNTs and ZnONRs can catalyze the electro-oxidation of H_2O_2, which sharply improves the sensitivity of the biosensor.

In order to reveal the optimal electrochemical responses of the presented biosensor, a comparative study was carried out by using four kinds of modified electrodes as: (a) ChOx/Pt–Au@ZnONRs/CS-MWCNTs/GCE, (b) ChOx/Pt–Au@ZnONRs/GCE, (c) ChOx/CS-MWCNTs/GCE and (d) CS-ChOx/GCE at an applied potential of 0.45 V with injecting the same concentration of cholesterol (40 μM). As shown in Fig. 7, the proposed biosensor ChOx/Pt–Au@ZnONRs/CS-MWCNTs/GCE showed the best chronoamperometric response. The reason was ascribed to the cooperation of the high catalytic activity for H_2O_2 electro-oxidation of Pt–Au@ZnONRs and CS-MWCNTs, therefore, ChOx/Pt–Au@ZnONRs/CS-MWCNTs/GCE exhibited a high electrocatalytic activity toward cholesterol.

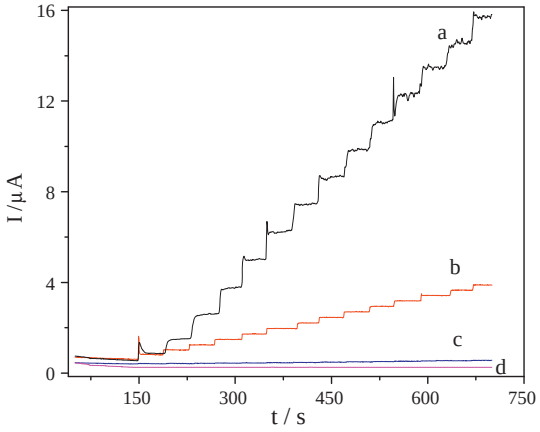

Fig. 7. Typical current–time response curves of different modified electrodes for successive addition of 40 μM cholesterol. (a) ChOx/Pt–Au@ZnONRs/CS-MWCNTs/GCE, (b) ChOx/Pt–Au@ZnONRs/GCE, (c) ChOx/CS-MWCNTs/GCE and (d) CS-ChOx/GCE. Test solution: stirring 0.05 M pH 7.0 PBS. Applied potential: 0.45 V.

3.6. Reproducibility, stability and anti-interference of the biosensor

The reproducibility of the proposed cholesterol biosensor was studied. Repetitive measurements were carried out in 5 mL PBS containing 0.1 mM cholesterol. The currents obtained in eight repeated measurements show a RSD of 2.4%, confirming that the measured results are reproducible. Thus, the film of CS-MWCNTs/Pt–Au@ZnONRs is efficient in retaining enzyme activity and the cholesterol biosensor has a good reproducibility.

The storage stability of the cholesterol biosensor was investigated in a period of 28 days. The response current to 0.1 mM cholesterol was tested every 2 days. When not in use, the electrode was suspended above 0.05 M PBS at 4 °C in a refrigerator. The enzyme electrode retained 82.5% of its original response current after 4 weeks, showing a longer lifetime. The good stability may be due to the fact that the CS-MWCNTs/Pt–Au@ZnONRs matrix provides an appropriate microenvironment for retaining the bioactivity of the enzyme molecules.

Under the optimized experiment conditions, the influence of the most common electrochemical interfering species (such as ascorbic acid, uric acid, L-cystine) to the current response of 0.2 mM cholesterol was investigated. Addition of 0.1 mM ascorbic acid, uric acid, L-cystine to 0.2 mM cholesterol solution had almost no observable interference on the current response of cholesterol (signal change below 3.8%). The result reveals that the cholesterol biosensor has good anti-interference ability.

3.7. Application in serum sample

To evaluate the ability of the biosensor for routine analysis, the biosensor was applied to the determination of cholesterol in blood serum samples. There was no pretreatment other than dilution of the samples. All of the concentrations of cholesterol determined were in the linear response range. As can be seen from Table 1, the results were satisfactory and agreed closely with those measured by the biochemical analyzer in the hospital. Analytical recovery rates of the glucose solution added to blood serum samples were

Table 1
Determination of cholesterol in blood serum samples.

Serum sample	Known value (μM)	Determined value[a] (μM)	RSD (%)	Relative deviation (%)	Cholesterol added (μM)	Cholesterol founded[a] (μM)	Recovery (%)
1	284.0	273.8 ± 7.39	2.70	−3.6	200.0	197.2 ± 6.51	98.6
2	426.0	431.5 ± 16.4	3.80	1.3	200.0	194.6 ± 2.92	97.3
3	430.0	449.4 ± 5.16	1.15	4.5	200.0	204.8 ± 5.73	102.4

[a] Average value from three determinations.

from 97.3 to 102.4%. These results indicate the reliability of this biosensor for cholesterol determination in real samples.

4. Conclusions

In summary, Pt–Au@ZnONRs could be synthesized by the method of multiple-step chemosynthesis, which is based on the bonding action of Au and NH_2 group of amino modified ZnONRs and the crystal seed function of the small size nano-Au in the formation of Pt shell on the functionalized ZnONRs. As to the amalgamation of the superiority of ZnONRs, nano-Pt and MWCNTs, the film of Pt–Au@ZnONRs/CS-MWCNTs can greatly increase the current response of the biosensor by loading more enzymes, providing a biocompatible environment for the ChOx and improving the catalyzed activity to the oxidation of H_2O_2 producing in the enzymatic reaction. Therefore, taking into account the good performance of the biosensor, the methodology employed in this study might be applied for the wide applications of biosensor in relation to the detection of H_2O_2.

Acknowledgments

This work was supported by the National Natural Science Foundation of China (21075100), Key Lab of Chongqing Modern Analytical Chemistry (201004), the Doctor Foundation of Southwest University (SWUB2008048) and the Fundamental Research Funds for the Central Universities (XDJK2009C082 and XDJK2012A004).

References

[1] J. MacLachlan, A.T.L. Wotherspoon, R.O. Ansell, C.J.W. Brooks, J. Steroid Biochem. Mol. Biol. 72 (2000) 169.
[2] A. Aghaei, M.R.M. Hosseini, M. Najafi, Electrochim. Acta 55 (2010) 1503.
[3] R.Z. Zhang, L. Li, S.T. Liu, R.M. Chen, P.F. Rao, J. Food Biochem. 23 (1999) 351.
[4] K. Hojo, H. Hakamata, A. Ito, A. Kotani, C. Furukawa, Y.Y. Hosokawa, F. Kusu, J. Chromatogr. A 1166 (2007) 135.
[5] K.W. Lin, Y.K. Huang, H.L. Su, Y.Z. Hsieh, Anal. Chim. Acta 619 (2008) 115.
[6] Y.C. Tsai, S.Y. Chen, C.A. Lee, Sens. Actuators B- Chem. 135 (2008) 96.
[7] Y. Wang, W.Z. Wei, X.Y. Liu, X.D. Zeng, Mater. Sci. Eng. C 29 (2009) 50.
[8] L.D. Zhu, J.L. Zhai, R.L. Yang, C.Y. Tian, L.P. Guo, Biosens. Bioelectron. 22 (2007) 2768.
[9] S. Hrapovic, Y.L. Liu, K.B. Male, J.H.T. Luong, Anal. Chem. 76 (2004) 1083.
[10] D.R.S. Jeykumari, S.S. Narayanan, Analyst 134 (2009) 1618.
[11] J.X. Wang, M.X. Li, Z.J. Shi, N.Q. Li, Z.N. Gu, Electroanalysis 14 (2002) 225.
[12] M.N. Zhang, K.P. Gong, H.W. Zhang, L.Q. Mao, Biosens. Bioelectron. 20 (2005) 1270.
[13] G. Li, J.M. Liao, G.Q. Hu, N.Z. Ma, P.J. Wu, Biosens. Bioelectron. 20 (2005) 2140.
[14] Y. Liu, X. Qu, H. Guo, H. Chen, B. Liu, S. Dong, Biosens. Bioelectron. 21 (2006) 2195.
[15] X.C. Tan, M.J. Li, P.X. Cai, L.J. Luo, X.Y. Zou, Anal. Biochem. 337 (2005) 111.
[16] P.R. Solanki, A. Kaushik, A.A. Ansari, A. Tiwari, B.D. Malhotra, Sens. Actuators B-Chem. 137 (2009) 727.
[17] J.F. Li, L.Z. Yao, W.L. Cai, J.M. Mo, Acta. Phys. Sin. 50 (2001) 1623.
[18] S.C. Navale, S.W. Gosavi, I.S. Mulla, Talanta 75 (2008) 1315.
[19] L.E. Greene, B.D. Yuhas, M. Law, D. Zitoun, P. Yang, Inorg. Chem. 45 (2006) 7535.
[20] Z.R. Dai, Z.W. Pan, Z.L. Wang, Adv. Funct. Mater. 13 (2003) 9.
[21] B. Liu, H.C. Zeng, J. Am. Chem. Soc. 125 (2003) 4430.
[22] A.B.F. Martinson, J.W. Elam, J.T. Hupp, M.J. Pellin, Nano Lett. 7 (2007) 2183.
[23] B. Liu, H.C. Zeng, Chem. Mater. 19 (2007) 5824.
[24] F.F. Zhang, X.L. Wang, S.Y. Ai, Z.D. Sun, Q. Wan, Z.Q. Zhu, Y.Z. Xian, L.T. Jin, K. Yamamoto, Anal. Chim. Acta 519 (2004) 155.
[25] J.E. Gregory, R. Aimee, Q.W. Li, F.W. Charles Jr., J. Vac. Sci. Technol. A 16 (1998) 1926.
[26] H. Gong, J.Q. Hu, J.H. Wang, C.H. Ong, F.R. Zhu, Sens. Actuators B- Chem. 115 (2006) 247.
[27] L.Y. Wang, Y. Sun, J. Wang, J. Wang, A.M. Yu, H.Q. Zhang, D.Q. Song, J. Colloid Interface Sci. 351 (2010) 392.
[28] Q. Wang, J.B. Zheng, Microchim. Acta 169 (2010) 361.
[29] M. Ahmad, C.F. Pan, L. Gan, Z.S. Nawaz, J. Zhu, J. Phys. Chem. C 114 (2010) 243.
[30] R. Manjunatha, D.H. Nagaraju, G.S. Suresh, J.S. Melo, S.F. D'Souza, T.V. Venkatesha, J. Electroanal. Chem. 651 (2011) 24.
[31] M.L. Guo, J.H. Chen, J. Li, L.H. Nie, S.Z. Yao, Electroanalysis 16 (2004) 1992.
[32] A. Umar, M.M. Rahman, M. Vaseem, Y.B. Hahn, Electrochem. Commun. 11 (2009) 118.
[33] A. Umara, M.M. Rahman, A. Al-Hajry, Y.B. Hahn, Talanta 78 (2009) 284.
[34] Q.C. Shi, T.Z. Peng, Y.N. Zhu, C.F. Yang, Electroanalysis 17 (2005) 857.
[35] B. Nikoobakht, M.A. El-Sayed, Chem. Mater. 15 (2003) 1957.
[36] A.S. Vengurlrkar, A.N. Chandorkar, K.V. Ramanathan, Thin Solid Films 114 (1984) 285.
[37] J.K. Gimxwhki, S. Veprck, Solid State Commun. 47 (1983) 747.
[38] C.D. Wagner, W.M. Riggs, L.E. Davis, J.F. Moulder, G.E. Muilenberg, Handbook of X-ray Photoelectron Spectroscopy, Physical Electronics Division, Perkin Elmer Corporation, Eden Prairie, Minnesota, 1979.
[39] S. Singh, P.R. Solanki, M.K. Pandey, B.D. Malhotra, Anal. Chim. Acta 568 (2006) 126.
[40] T. Yao, K. Takashima, Biosens. Bioelectron. 13 (1998) 67.
[41] C.C. Allain, L.S. Poon, C.S.G. Chan, W. Richmond, P.C. Fu, Clin. Chem. 20 (1974) 470.
[42] C.S.P. Suman, Curr. Appl. Phys. 3 (2003) 129.
[43] A.I. Gopalan, K.P. Lee, D. Ragupathy, Biosens. Bioelectron. 24 (2009) 2211.
[44] Y.T. Lin, S.S. Wu, H.L. Wu, J. Chromatogr. A 1156 (2007) 280.
[45] C. Dhand, S.K. Arya, M. Datta, B.D. Malhotra, Anal. Biochem. 383 (2008) 194.
[46] R.S. Dey, C.R. Raj, J. Phys. Chem. C 114 (2010) 21427.